CHEMISTRY OF MATERIALS

ARTICLE

pubs.acs.org/cm

Covalently Assembled Gold Nanoparticle-Carbon Nanotube Hybrids via a Photoinitiated Carbene Addition Reaction

Hossein Ismaili, François Lagugné-Labarthet, and Mark S. Workentin*

Department of Chemistry, The University of Western Ontario, London, Ontario ON N6A 5B7, Canada

Supporting Information

ABSTRACT: A nanohybrid consisting of monolayer protected gold nanoparticles (AuNPs) covalently attached to multiwalled carbon nanotubes (CNT) was prepared using a photoinitiated carbene addition approach. Photolysis of 3-aryl-3-(trifluoromethyl)diazirine-modified gold nanoparticles (Diaz-AuNPs) of two core sizes (3.9 ± 0.9 nm and 1.8 ± 0.3 nm in diameter) resulted in the generation of reactive carbene intermediates on the monolayer of the AuNPs. In the presence of untreated CNT the reactive carbenes undergo an addition reaction with the π-conjugated carbon skeleton. The AuNPs are well dispersed on the sidewall of the CNT and the hybrids are robust enough to survive vigorous washing in a variety of solvents. In the absence of photolysis no covalent attachment occurs with the same AuNP. The nanohybrid AuNP-CNTs were characterized using transmission electron microscopy (TEM), X-ray diffraction (XRD), Raman, and UV−visible spectroscopy. All of the characterization studies confirm the presence of the AuNPs. This methodology provides support that this photoinitiated carbene reactivity can be utilized for the functionalization of other materials with nanoparticles.

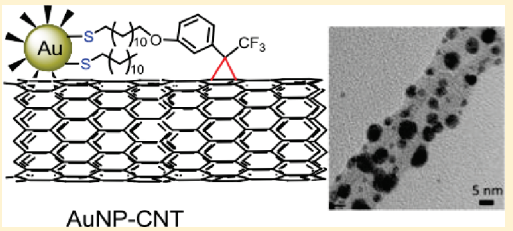

KEYWORDS: nanomaterials, nanoparticles, nanotubes, photosensitive materials, hybrid inorganic/organic materials

INTRODUCTION

Monolayer-protected gold nanoparticles (AuNPs)[1] and carbon nanotubes (CNTs)[2] are arguably the two most common nanosized building blocks for current materials applications. The former are one of the most stable metal nanoparticles, easy to synthesize in a variety of core sizes; there is a protocol to modify these AuNP with additional functionality, and they possess attractive electrochemical and optical properties.[3,4] The latter, since their discovery in 1991,[5] have been central to the development of hybrid nanomaterials because of their outstanding mechanical, optical, electrical, and thermal properties.[6] With the aim to capitalize on the features of both of these types of materials for applications in areas as diverse as chemical and biochemical catalysis,[3] sensors,[4] development of fuel cells,[7] and transistors,[8] there has been much recent effort to fabricate nanohybrids where the CNT acts as a support for a variety of noble metal nanoparticles (NP), such as AgNP, PtNP, and AuNP.[9] Applications of nanoparticle-carbon nanotube (NP-CNT) hybrids require the development of methods for their preparation that lead to robust structures without significantly compromising the integrity of the underlying CNT framework. Thus preparing covalent NP-CNT hybrids with uniform dispersion of the nanoparticles onto the CNT and tuning the size of nanoparticles remain important challenges of NP-CNT hybrids fabrication and applications.

Generally there are three main strategies that are utilized to deposit noble metal NP and specifically AuNP onto the surface of CNT. These broadly can be classified as covalent approaches, non-covalent approaches, and direct formation of AuNPs.[9] In the direct formation method, naked AuNP (those AuNP that do not have a stabilizing monolayer ligand) are grown on the CNTs using methods such as chemical vapor deposition,[10] electrodeposition,[11] and thermal decomposition.[12] This approach is limited because of the need for more complex instrumentation, the often slow deposition rate, and more importantly, the lack of control over AuNP size.[6,10−12] Furthermore, AuNP formed in this way are also more unstable and undergo agglomeration losing control of the dispersity of the AuNP on the CNT.

Non-covalent approaches are also utilized to prepare AuNP-CNT nanohybrids. Here the preparation utilizes one or more of hydrophobic,[13] electrostatic,[14] van der Waals[15] as well as $\pi-\pi$ stacking[16] interactions between the native or treated CNT and functionality on the monolayer protected AuNPs. The advantages of these methods are that they allow for the reversible preparation of protected metal AuNP-CNT hybrids and do not lead to any destructive interactions on the integrity of the chemical structure of the CNT sidewalls. However, because the interactions are inherently weaker than covalent bonds, the AuNPs on the surface of CNTs are not robust and thus may easily disassemble, often by simple washing of the AuNP-CNT hybrids.

For many applications a covalent interaction between the monolayer protected AuNP and the CNT is beneficial. Covalent attachment offers several advantages: (i) because the AuNPs are synthesized in advance, the size and shape of the AuNP is

Received: November 15, 2010
Revised: January 18, 2011
Published: February 11, 2011

dx.doi.org/10.1021/cm103284g | *Chem. Mater.* 2011, 23, 1519–1525

Scheme 1. Illustration of the Reaction Protocol Utilized for the Functionalization of CNT with Diazirine-Modified AuNPs (Diaz-AuNPs)

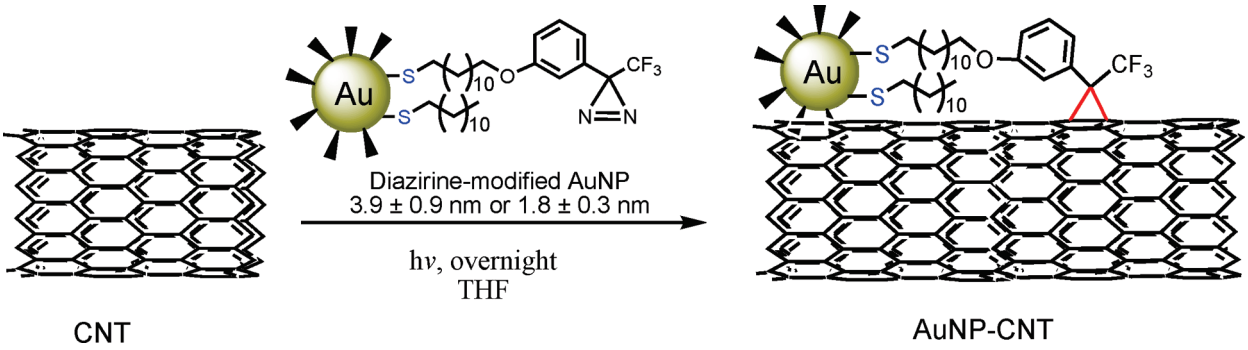

controlled by well-known procedures; (ii) using covalent bonds leads to formation of more robust nanohybrids from which the AuNP will not easily be displaced; and (iii) the loading efficiency of AuNP onto the CNTs can be tailored via variation of AuNP concentration.[9b,9c,17] Most approaches to date for the preparation of covalently assembled AuNP-CNT hybrids requires the chemical pretreatment of the CNT surface to expose functionality that can be further elaborated, for example with a functional molecule containing a terminal thiol group, which is then utilized to form the bond with the AuNP. The first step of functionalization is often the oxidation of the CNT, which usually requires aggressive acid treatment, high temperature, and sonication.[6a,18] The pretreatments often damage the structural integrity of the CNT and adversely affect their electrical and mechanical properties. Fracture of the CNT, formation of holes in the sidewalls, successive removal of the graphene cylinders (in the case of multiwalled CNTs), as well as functionalization of only defect sites are observed under these aggressive conditions.[6a,19]

Given these approaches, it remains a desirable goal to develop efficient strategies for the formation of AuNP-CNT nanohybrids through covalent assembly, while also avoiding the need to pretreat/modify the surface of CNTs and to take advantage of the ability to prepare the AuNP with known core size prior to its incorporation onto the CNT. Carbene and nitrene addition reactions were among the first employed to modify CNTs.[20] Chen and co-workers reported the chemical functionalization of CNTs using nucleophilic addition of dichlorocarbene generated from different precursors, including mercury complex[20a] and $CHCl_3$/NaOH.[20b] In addition, photolysis and thermolysis of an azide functionality incorporated on a variety of different platforms to yield reactive nitrenes has been utilized to functionalize CNTs.[20c] In a recent example, McCall and co-workers took advantage of the photoreactivity of azidothymidine and the resulting nitrene chemistry to modify CNT which can be further elaborated to decorate the CNT with DNA to produce water-soluble CNTs.[20d] Bai and co-workers used similar photoinitiated nitrene chemistry of an azide copolymer to coat the surface of CNTs.[20e]

Photogenerated carbene reactivity has not been utilized like those of the nitrene reactions for the modification of CNT sidewall surfaces even though they offer many of the same advantages. In this report we utilize a photogenerated carbene to modify multiwalled CNTs with AuNPs. The carbene addition approach allows direct coupling of the carbene carrier onto the π-conjugated carbon skeleton of CNT. Our strategy involves the generation of a reactive carbene intermediate directly on the monolayer of an AuNP and to utilize its subsequent addition reaction onto the π-backbone of CNT for covalent coupling of AuNP to the CNT, with no need for oxidizing the surface of CNTs. We recently reported the synthesis and modification of 3-aryl-3-(trifluoromethyl) diazirine-modified AuNPs (Diaz-AuNP) through photoinduced carbene insertion reactions.[21] We demonstrated that upon irradiation of the diazirine group tethered onto the AuNP, an intermediate carbene is generated by photoinitiated nitrogen extrusion, and insertion reactions then occurred in the presence of a selection of reactants with X-H (X: O, N) and alkene functional groups. Herein, we report that the irradiation of similar Diaz-AuNP in the presence of multiwalled CNTs leads to covalent assembly of the AuNP onto the CNT by means of a carbene addition approach (Scheme 1). We investigated this approach by using two different Au core sizes of Diaz-AuNP: Lg-Diaz-AuNP with a larger, yet more disperse core size (3.9 ± 0.9 nm) was used initially to maximize sensitivity for our characterization techniques and optimize reaction conditions, and then the method was extended to a Sm-Diaz-AuNP with a smaller core size (1.8 ± 0.3 nm in diameter). The approach allows for facile formation of robust AuNP-CNT nanohybrids in a single step without the need to pre-functionalize the CNT.

EXPERIMENTAL SECTION

Commercial Solvents and Reagents Used. Deuterated chloroform ($CDCl_3$) and dichloromethane (CD_2Cl_2) (Cambridge Isotope Laboratories) were used as received. The compounds dodecanethiol, hydrogen tetrachloroaurate(III), tetraoctylammonium bromide (TOAB), 1,12-dibromododecane, 3-bromoanisole, *n*-butyllithium, hydroxylamine hydrochloride, (*N*,*N*-dimethylamino) pyridine, *p*-toluenesulfonylchloride, silver(I) nitrate, boron tribromide, potassium thioacetate, acetyl chloride, and multiwalled carbon nanotubes (Alfa Aesar, 95% purity, 20 nm OD, 5−20 μm long) were used as received from the suppliers.

General Instrumentation. ^{1}H, ^{13}C, and ^{19}F NMR spectra were recorded on either a Varian Inova or Mercury 400 spectrometer (^{1}H: 400 MHz, ^{13}C: 100 MHz, and ^{19}F: 376 MHz) and chemical shifts are reported in parts per million (ppm) relative to internal TMS (0.00 ppm) or the signals from the NMR solvent ($CHCl_3$: δ 7.26 ppm for ^{1}H NMR, δ 77.0 ppm for ^{13}C NMR; and $CFCl_3$: δ 0 ppm for ^{19}F NMR). Mass spectra and exact mass were recorded on a MAT 8200 Finnigan High Resolution Mass Spectrometer. Infrared spectra were recorded on a Bruker Vector 33 FTIR spectrometer and are reported in wavenumbers

Scheme 2. Synthetic Procedure Used in the Preparation of Lg-Diaz-AuNPs

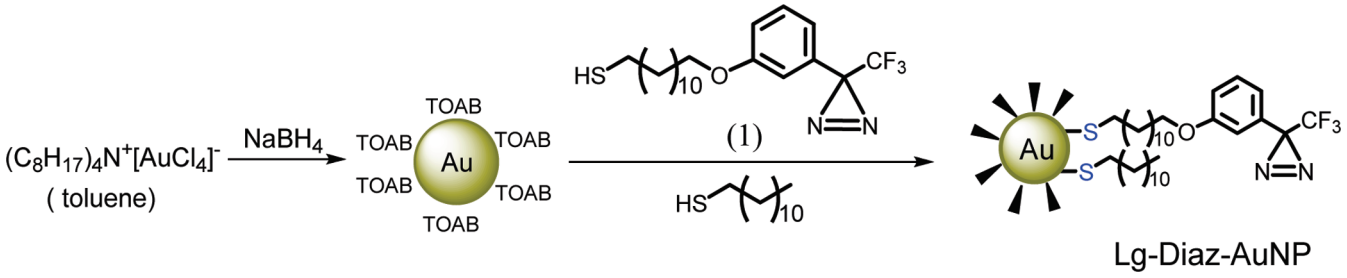

(cm^{-1}). The light source used for the photochemical reactions was a Hanovia medium pressure mercury lamp (PC 451050/805221). Transmission electron microscopy (TEM) images were recorded on a Philips CM-10 TEM operating at 100 kV and FEI Tecnai G2 F20 operating at 200kv. UV−visible absorption spectra were recorded on a Cary 100 spectrometer in spectroscopic grade tetrahydrofuran (THF) and CH_2Cl_2. An Inel MPD (Multi-Purpose Diffractometer) with a curved CPS 120 detector was used to collect X-ray powder diffraction data (XRD). The pattern was taken in the range of 5 and 120 degrees 2θ with copper radiation. Raman spectra were acquired with a Horiba-Jobin-Yvon Labram HR confocal microscope with a 800 mm focal length, a 600 grooves per mm grating and a CCD detector cooled with liquid nitrogen. The excitation wavelength was set to λ = 632.8 nm, and the spectrometer was calibrated against a silicon wafer reference. A 100×, 0.9 numerical aperture microscope objective was used to focus the excitation beam ($\phi \approx 1$ μm at the focal point) on a bundle of carbon nanotubes. Acquisition time was set to 40 s for each measurement. The carbon nanotubes were deposited onto pristine fused-silica coverslips (0.2 mm thick) for the Raman experiments.

Synthesis of Large-Diazirine-Modified AuNPs (Lg-Diaz-AuNP, 3.9 ± 0.9 nm). Lg-Diaz- AuNP were prepared using a modified two phase Brust-Schiffrin method (Scheme 2).[22−24] Hydrogen tetrachloroaurate (III) trihydrate (88.6 mg, 0.24 mmol) was dissolved in 7.5 mL of distilled water (resulting in a bright yellow solution) and then added to a solution of tetraoctylammonium bromide (TOAB) (0.574 g, 1.05 mmol) in 21 mL toluene. The contents were stirred for 20 min at room temperature to facilitate the phase transfer of the hydrogen tetrachloroaurate (III) trihydrate into the toluene layer. After phase transfer, the aqueous layer was removed and a fresh solution of sodium borohydride (90.8 mg, 2.4 mmol) in 12 mL water was slowly added to the vigorously stirring toluene solution over 10 min. The reaction mixture was stirred for 2h and then the aqueous layer was removed. Dodecanethiol (93 mg, 0.46 mmol) and diazirinethiol (**1**) (93 mg, 0.23 mmol), synthesized as previously reported,[21] were added to the solution and stirred overnight. The wine red toluene layer was washed with 3 × 10 mL of distilled water and evaporated to reduce the volume to ~2 cm^3. The resulting Lg-Diaz- AuNPs were suspended in 100 mL of 95% ethanol and placed in the freezer overnight during which time they precipitated from the solution. The supernatant was decanted, and the precipitate was dissolved in 100 mL of toluene/ethanol (2:3 v/v) and sonicated for 1 min and reprecipitated. The dissolving and reprecipitation procedure was repeated five times. The Lg-Diaz-AuNP mixture was evaporated to dryness, dissolved in toluene, and stored in the freezer. The product was characterized by ^{1}H NMR, ^{19}F NMR, and UV−visible spectroscopy and TEM (Supporting Information).

Synthesis of Small-Diazirine-Modified AuNPs (Sm-Diaz-AuNPs, 1.8 ± 0.3 nm). Hydrogen tetrachloroaurate (III) trihydrate (0.30 g, 0.77 mmol) was dissolved in 28 mL of distilled water and then mixed with tetraoctylammonium bromide (2.30 g, 4.2 mmol) in 70 mL of toluene. The contents were stirred for 30 min at room temperature resulting in the organic layer turning to a dark orange color and the aqueous layer becoming clear and colorless. After phase transfer, the aqueous layer was removed and the organic layer was cooled to 0 °C in ice bath. Dodecanethiol (0.468 g, 0.57 mL, 2.31 mmol) was added to the solution via a volumetric pipet and stirred for 10 min. The addition of dodecanethiol resulted in a color change from brownish-orange to clear and colorless. A fresh solution of sodium borohydride (0.33 g, 8.7 mmol) in 28 mL water was then added to the rapidly stirring toluene solution over 5 s. The solution darkened instantly, eventually becoming dark brown. The mixture stirred overnight (~18 h) as it warmed to room temperature. After this time the aqueous layer was removed and the toluene layer was washed with 3 × 20 mL of distilled water and dried over $MgSO_4$, filtered, and evaporated to dryness. The product, small AuNPs, was suspended in 200 mL of 95% ethanol and placed in the freezer overnight during which time the nanoparticles precipitated from solution. When the small AuNPs had precipitated, the supernatant was decanted, and the precipitate was dissolved in benzene and concentrated, resulting in the formation of a film in the round-bottom flask. This film was washed repeatedly with 10 × 15 mL of 95% ethanol, resulting in pure small AuNPs as judged by ^{1}H NMR spectroscopy, which showed no signs of free dodecanethiol, dodecyldisulfide, or tetraoctylammonium bromide. Small AuNPs (200 mg) were dissolved in 25 mL of toluene and degassed with nitrogen. Diazirinethiol (**1**) (206 mg, 0.51 mmol) was added to the small AuNP solution in toluene and stirred for 20 h at room temperature. The solvent was evaporated, and the resulting dark film (Sm-Diaz-AuNP) was washed with 95% ethanol and dried.

Synthesis of Dodecanethiolate-AuNP (Model-AuNP, 4.9 ± 0.9 nm). Model-AuNPs (without the diazirine functionality) were prepared as described for Lg-Diaz-AuNP except that only the dodecanethiol was used as a protecting ligand.

Decoration of CNTs with Lg-Diaz-AuNP (Lg-Diaz-AuNP-CNT) or Sm-Diaz-AuNP (Sm-Diaz-AuNP-CNT). Multiwalled CNTs (~ 1 mg) were dispersed in 10 mL of THF using sonication (5 min). Lg-Diaz-AuNP or Sm-Diaz-AuNP (10 mg) were dissolved in 2 mL of THF and added to the CNTs suspension. The mixture was placed in a Pyrex test tube, degassed with argon for 15 min, and irradiated using a medium pressure mercury lamp (Hanovia PC 451050/805221) at room temperature for 15 h while stirring. Then the CNTs decorated with AuNPs were isolated by centrifugation. The product, Lg-Diaz-AuNP-CNT or Sm-Diaz-AuNP-CNT, was subjected to exhaustive centrifugation and washing cycles using THF, toluene, and chloroform to remove the excess and unreacted AuNP.

Control experiments included (a) stirring a solution of Lg-Diaz-AuNP and multiwalled CNTs in THF in the absence of light and subjecting the CNTs to the same workup procedures as that the irradiated and (b) irradiation of a mixture of dodecanethiol modified-AuNP (Model-Au-NP, that is, without diazirine ligand) and multiwalled CNTs in THF under the identical conditions as described above.

dx.doi.org/10.1021/cm103284g |*Chem. Mater.* 2011, 23, 1519–1525

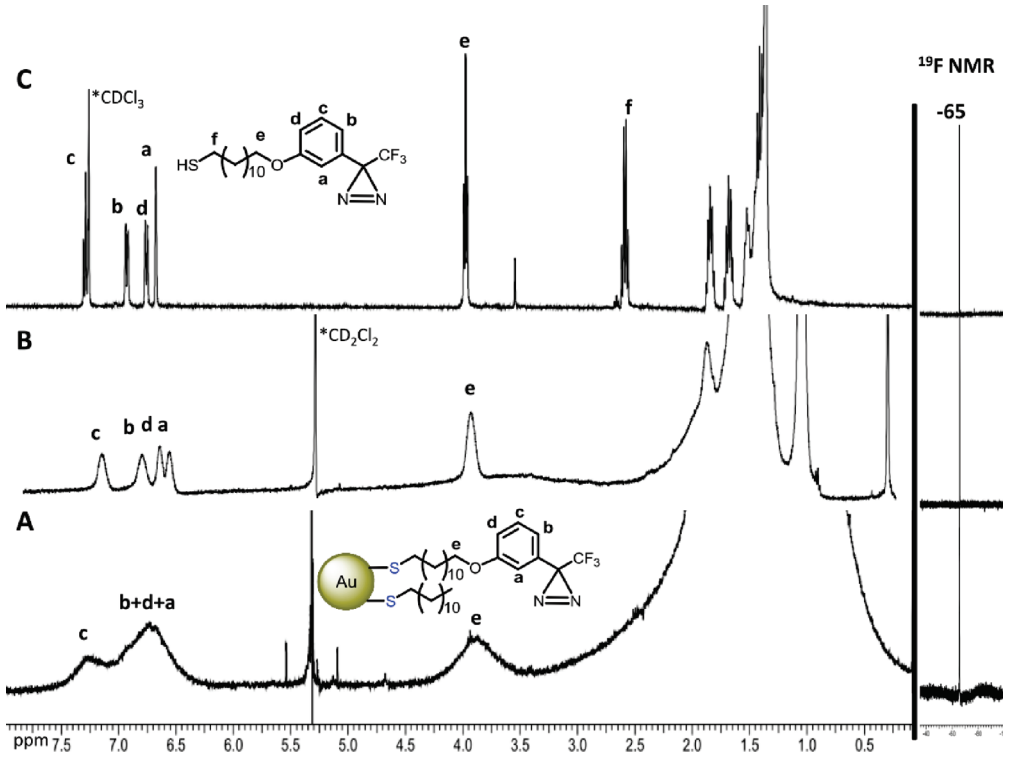

Figure 1. ^{1}H NMR and ^{19}F NMR spectra of (A) Lg-Diaz-AuNPs, (B) Sm-Diaz-AuNPs, and (C) diazirinethiol **1**. The ^{19}F NMR are on the far right.

RESULTS AND DISCUSSION

The diazirinethiol (**1**) and Sm-Diaz-AuNPs (1.8 ± 0.3 nm) were synthesized according to a previously reported procedure.[21] The Lg-Diaz-AuNPs (3.9 ± 0.9 nm) were synthesized using a modified two-phase Brust−Schiffrin method (Scheme 2).[22−24] In this preparation procedure tetraoctylammonium bromide (TOAB)-stabilized AuNPs were made by reducing Au^{3+} with $NaBH_4$ in the presence of TOAB. In the next step, TOABs were place-exchanged with diazirinethiol (**1**) and dodecanethiol affording Lg-Diaz-AuNPs. The product Lg-Diaz-AuNPs were characterized by ^{1}H NMR, ^{19}F NMR, and UV−visible spectroscopy and TEM. The average Au core diameter of Lg-Diaz-AuNPs prepared in this way was 3.9 ± 0.9 nm with a distribution range of 2.6−6 nm, as determined by TEM (Supporting Information, Figure S1).

^{1}H NMR spectroscopy is a powerful tool for characterizing and monitoring the purity of functionalized AuNPs. The ^{1}H NMR spectra of Lg-Diaz-AuNP and Sm-Diaz-AuNP (Figure 1A and B, respectively) show broad peaks at 0.7−2.25 ppm assignable to the methylene and methyl groups of diazirinethiolate (**1**) and dodecanethiolate attached onto the AuNP core. A broad peak centered at 3.90 (e) ppm is due to the methylene alpha to the oxygen of (**1**), and broad peaks at 6.50−7.05 (a, b, and d) and 7.28 (c) ppm are assigned to the aromatic hydrogens of the aromatic ring. It should be noted that the ^{1}H NMR spectrum of ligands on larger size particles is characterized by broader signals. Figure 1C shows the ^{1}H NMR spectrum of free (**1**). As can be seen, good alignment of the chemical shifts between (**1**) and the two Diaz-AuNPs in Figure 1 signifies the successful exchange reaction and incorporation of (**1**) onto the AuNP. The lack of sharp signals in the ^{1}H NMR spectra of the Diaz-AuNPs confirms the purity of product AuNPs otherwise the sharp peaks due to impurities such as unbound (**1**), dodecanethiol, or TOAB would appear. In addition, we employed ^{19}F NMR spectroscopy to characterize the Diaz-AuNPs. The ^{19}F NMR spectrum of the two Diaz-AuNPs shows a single peak at −65 ppm assignable to the fluorine of the CF_3 group of (**1**), a further indication of incorporation of (**1**) onto the AuNP (Figure 1).[21]

The UV−visible spectrum of Lg-Diaz-AuNP exhibits a broadened surface plasmon band centered around 530 nm, characteristic of AuNP with a core size >3 nm. The Sm-Diaz-AuNPs do not show the plasmon band. Both the Lg-Diaz and Sm-Diaz-AuNP have a stronger absorption between 270 and 350 compared to the absorption of Model-AuNP as expected for the incorporation of the diazirine chromophore onto the AuNP (Supporting Information, Figure S2).

Scheme 1 illustrates the photochemical approach utilized for the covalent attachment of the Diaz-AuNP onto the CNT. As stated, irradiation of terminal diazirine group that is attached onto the Diaz-AuNP creates a reactive carbene at the interface of the AuNP after nitrogen extrusion. The subsequent carbene then adds onto the sidewall of the CNT via a carbene nucleophilic addition. In a typical procedure, 1 mg of as-received multiwalled CNTs with 95% purity was dispersed in 10 mL of THF. A solution of Lg-Diaz-AuNP or Sm-Diaz-AuNP in THF (5 mg/1 mL) was added to the CNTs suspension in a septum sealed Pyrex test tube, and the solution was purged with argon. The system was irradiated using a medium pressure mercury lamp at room temperature for 15 h. The resulting AuNP-CNT nanohybrid was isolated by repeated centrifugation and washing using THF, $CHCl_3$, and toluene to remove any unbound AuNPs. A drop of the obtained nanohybrid was dispersed in THF and cast onto a copper grid (300 mesh, coated with carbon film) for TEM investigations. As evident in Figure 2, Lg-Diaz-AuNP and Sm-Diaz-AuNP are bound to the sidewall of the CNTs with a rather even distribution. Figures 2A and 2B show the HRTEM and

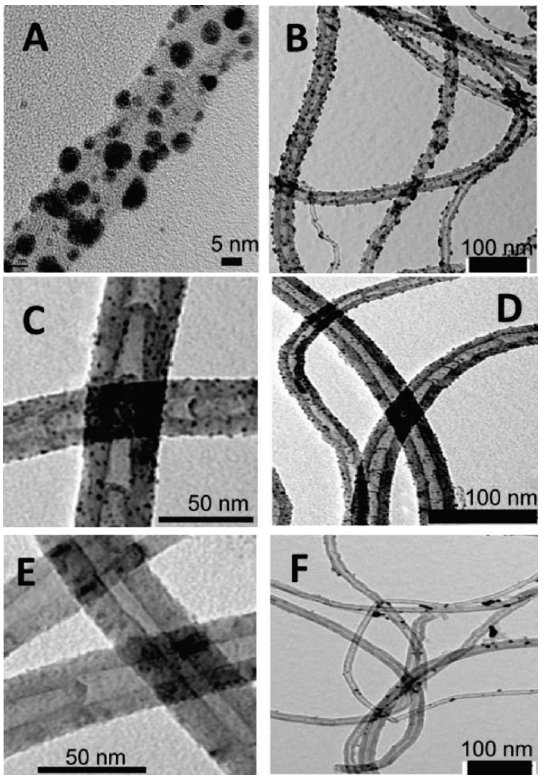

Figure 2. TEM images of CNTs after photoreaction and washing/purification protocol (A, B) photoreaction with Lg-Diaz-AuNPs (Lg-Diaz-AuNP-CNT); (C, D) photoreaction of Sm-Diaz-AuNPs (Sm-Diaz-AuNP-CNT); (E, F) CNTs exposed to the same solutions as A/B but in the absence of UV−visible irradiation and after the washing/purification protocol.

TEM images of Lg-Diaz-AuNP-CNT, respectively, and TEM images of Sm-Diaz-AuNP-CNT are shown in Figures 2C and 2D. It is important to note that the AuNPs were stable under UV irradiation, and no noticeable change was observed in the shape or size of the Au core after irradiation.

To provide support for the role of the carbene addition in forming the AuNP-CNT nanohybrid via covalent assembly, we carried out two set of control experiments. The first was stirring a solution of Lg-Diaz-AuNP and CNTs in the absence of irradiation. The Lg-Diaz-AuNP contain alkane chains and aromatic rings, therefore non-covalent interactions including weak van der Waals and $\pi-\pi$ stacking can also engage in the assembly of a nanohybrid. Because these samples were not irradiated the diazirine groups remained intact and no carbenes were formed. In this case, only non-covalent interactions would lead to the formation of an AuNP-CNT nanohybrid. However, TEM images taken of the solid material, after the same centrifugation and washing cycle protocol (see Experimental Section), showed just bare CNT with no AuNP attached onto the nanotubes (Figure 2E and 2F). In addition, to verify the requirement for irradiation in the nanohybrid formation, a mixture of Model-AuNPs (i.e., those without incorporation of the diazirine ligand (**1**) onto the AuNP) and CNT was exposed to the same irradiation and purification protocol conditions described above. The TEM of the obtained material showed only CNT with no AuNP incorporated onto them. The conclusion of these control experiments is that UV irradiation of the diazirine moiety

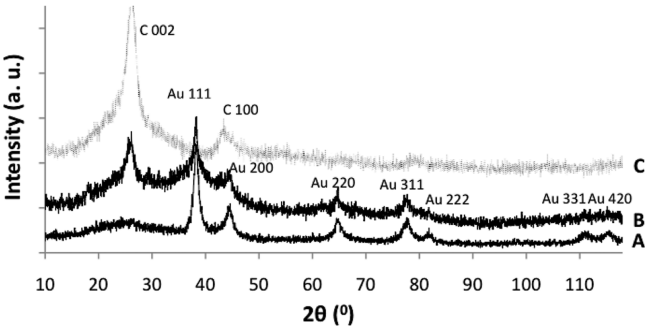

Figure 3. XRD patterns of (A) Lg-Diaz-AuNP-CNT, (B) Sm-Diaz-AuNP-CNT, and (C) pure CNT.

incorporated on the AuNP to generate the intermediate carbene and its subsequent nucleophilic addition is responsible for the covalently assembled AuNP-CNT nanohybrid.

The Diaz-AuNPs have the reactive ligand roughly equally distributed on the surface and for the formation of the nanohybrid only one (or at most a few) carbene additions are expected. One question that arises is what is the fate of the carbene intermediates generated away from the CNT surface? We suspect that carbenes that do not covalently react with the CNTs react with solvent, in this case THF, albeit at a much slower rate than addition to the CNT, an observation we made previously.[21] Another possible fate is for the carbenes to react with the carbenes (or ligands) on another AuNP. However, the TEM shows no real evidence for agglomeration of AuNPs because of dimerization of carbenes or reaction of a carbene ligand on one AuNP with another.

To further identify the presence of the AuNP on the surface of the CNT the AuNP-CNT nanohybrids were characterized using X-ray diffraction (XRD). The XRD of the Lg-Diaz-AuNP-CNT and Sm-AuNP-CNT nanohybrids are shown in Figure 3. The (111), (200), (220), (311), (222), (331), and (420) are planes of a face-centered cubic (fcc) AuNP, affirming the presence of AuNP in the nanohybrids.[25] The C (002) plane of carbon nanotubes is absent in the XRD spectrum of Lg-Diaz-AuNP-CNT but is present in the XRD spectrum of Sm-Diaz-AuNP-CNT. The surface coverage of the AuNP on the Lg-Diaz-AuNP-CNT is higher than that on the Sm-Diaz-AuNP-CNT; therefore, the X-ray beam does not efficiently interrogate the surface of nanotubes in the Lg-Diaz-AuNP-CNT, and planes due to C (200) cannot be observed as readily in the XRD pattern of these samples.

Further characterization of the AuNP-CNT nanohybrids was done using Raman spectroscopy. Raman spectra were measured using two different laser wavelengths, namely, a 514 nm and a 632 nm laser. As reported previously the D/G ratios observed for the unmodified CNT vary with the excitation wavelength,[26] and in the present case this ratio was 0.9 using the 514 nm laser and 1.19 using the 632 nm laser. Raman spectra of the AuNP-CNT hybrids could only be measured using the 632 nm laser, because excitation using the 514 nm laser leads to a visible thermal decomposition of the sample. This is likely due to the thermal energy produced on excitation at the plasmon absorption band in the AuNP; we are currently investigating the practical applications of this observation further. The spectra obtained for the Lg-Diaz-AuNP-CNT and unmodified CNT measured using the 632 nm laser are shown in Figure 4. The peaks at 1315 and 1567 cm^{-1} are

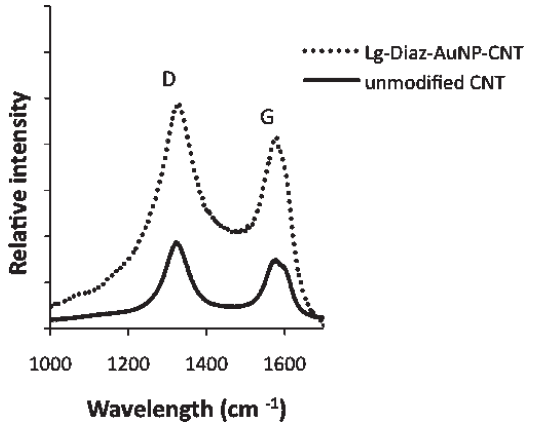

Figure 4. Raman spectra of Lg-Diaz-AuNP-CNT (dashed line) and unmodified CNT (solid line).

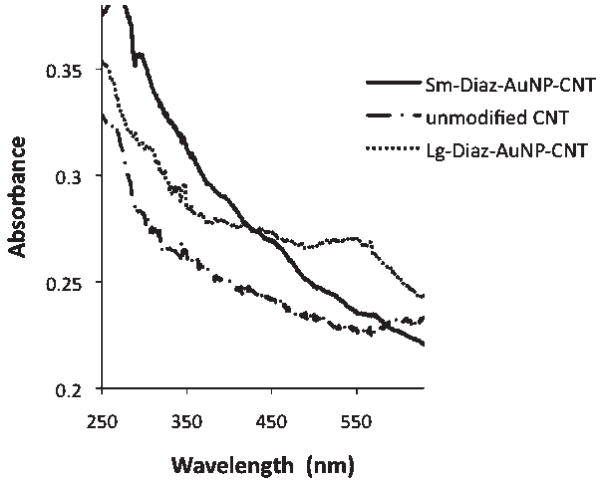

Figure 5. UV−visible absorption spectra of unmodified CNT, Sm-Diaz-AuNP-CNT, and Lg-Diaz-AuNP-CNT. The latter clearly exhibits the Plasmon absorption band.

the D and G bands of CNTs, respectively.[16] A Raman enhancement of a factor of approximately three was observed with the Lg-Diaz-AuNPs; Au-NP are well-known to enhance the Raman signal of these bands. It is noteworthy that the R values (intensity ratio of D/G band) of CNT (R = 1.21) and AuNP-CNT nanohybrid (R = 1.19) did not considerably change, suggesting that the carbene addition reaction did not significantly affect the underlying structure of the CNT. The same Raman enhancement was not observed in the case of Sm-Diaz-AuNP-CNT. The Small AuNPs do not exhibit a strong surface plasmon band in its UV−visible spectrum that is the main contribution to the surface-enhanced Raman scattering.[27]

The UV−visible spectra of the CNT, Lg-Diaz-AuNP-CNT, and Sm-Diaz-AuNP-CNT provide additional support for the incorporation of the AuNP (Figure 5). The appearance of the surface plasmon band in the UV−visible spectrum of Lg-Diaz-AuNP-CNT implies the presence of the AuNPs onto the CNT. The surface plasmon band of AuNPs in the Lg-Diaz-AuNP-CNT nanohybrid is broader and red-shifted (from 530 to 555 nm) compared with that of unreacted Lg-Diaz-AuNP. It has been suggested that the red shift of the surface plasmon band is because of interparticle interactions of AuNPs attached onto the CNTs, as well as the lowering of energy states of the AuNPs because of their interaction with the CNTs.[28]

CONCLUSIONS

The photoinitiated carbene generated from diazirine-modified AuNPs (Diaz-AuNPs) allows for the efficient covalent attachment of AuNP onto multiwalled CNT. On the basis of our earlier studies, we believe this presumably occurs via carbene addition to the native graphitic surface of the CNT. The reactions proceed efficiently with as received CNT, without the need for pretreatment of the CNT to incorporate additional surface functionality on the CNT. Pretreatment of CNT via some oxidative procedure is often used to purify the CNT while also introducing oxygen-containing functionality such as hydroxy or carboxyl surface groups that helps with the exfoliation of CNT bundles and solubility. In the present study, any such pretreatment would lead to even greater reactivity because the carbenes generated were shown to react more efficiently by insertion into O−H bonds.[21]

The monolayer ligands of the AuNP that remain exposed in the AuNP-CNT nanohybrid can, in principle, undergo place-exchange reactions with other thiol ligands. In situ place exchange reactions provide a plausible method to tailor or adjust the solubility characteristics or other features of these AuNP-CNT nanohybrids.

The high reactivity of the generated carbene intermediates toward insertion and addition reactions suggests that the approach described here can be used to incorporate suitably diazirine-derivatized AuNP (and indeed other metal-NP) to other materials containing a variety of native or synthesized surface functionality. Because the mode of attachment of the AuNP is through photochemical activation, the methodology can be combined with photolithographic techniques to produce patterns of the metal NP on these surfaces; we are currently investigating the breadth of materials that can be modified using the methodology described.

ASSOCIATED CONTENT

Supporting Information. TEM image of Lg-Diaz-AuNP and the absorption spectra of Model-AuNPs, Lg-Diaz-AuNPs, Sm-Diaz-AuNPs and diazirinethiol **1**. This material is available free of charge via the Internet at http://pubs.acs.org.

AUTHOR INFORMATION

Corresponding Author
*E-mail: mworkent@uwo.ca.

ACKNOWLEDGMENT

This research is supported by the Natural Sciences and Engineering Research Council of Canada discovery grants program (NSERC-DG). Robert Harris at the Advanced Analysis Centre at the University of Guelph (TEM), Richard Harris at the Western Biotron (TEM), Dr. German Popov (XRD), and Nastaran Kazemi (Raman) are thanked for their technical expertise.

REFERENCES

(1) (a) Giljohann, D. A.; Seferos, D. S.; Daniel, W. L.; Massich, M. D.; Patel, P. C.; Mirkin, C. A. *Angew. Chem., Int. Ed.* **2010**, *49*, 3280. (b) Boisselier, E.; Astruc, D. *Chem. Soc. Rev.* **2009**, *38*, 1759. (c) Wilson, R. *Chem. Soc. Rev.* **2008**, *37*, 2028. (d) Ghosh, S. K.; Pal, T. *Chem. Rev.* **2007**, *107*, 4797.

(2) *Carbon nanotube and related structures: synthesis, characterization, functionalization, and applications*; Guldi, D. M., Martin, N., Eds.; Wiley-VCH: Weinheim, Germany, 2010.

(3) (a) Schatz, A.; Reiser, O.; Stark, W. J. *Chem.—Eur. J.* **2010**, *16*, 8950. (b) Chen, M.; Goodman, D. W. *Chem. Soc. Rev.* **2008**, *37*, 1860.

(4) (a) Wang, Z.; Ma, L. *Coord. Chem. Rev.* **2009**, *253*, 1607. (b) Stewart, M. E.; Anderson, C. R.; Thompson, L. B.; Maria, J.; Gray, S. K.; Rogers, J. A.; Nuzzo, R. G. *Chem. Rev.* **2008**, *108*, 494.

(5) Iijima, S. *Nature* **1991**, *354*, 56.

(6) (a) Eder, D. *Chem. Rev.* **2010**, *110*, 1348, and references therein. (b) Wu, H. C.; Chang, X.; Liu, L.; Zhao, F.; Zhao, Y. *J. Mater. Chem.* **2010**, *20*, 1036.

(7) Chu, H.; Wei, L.; Cui, R.; Wang, J.; Li, Y. *Coord. Chem. Rev.* **2010**, *254*, 1117.

(8) Dong, X.; Lau, C. M.; Lohani, A.; Mhaisalkar, S. G.; Kasim, J.; Shen, Z.; Ho, X.; Rogers, J. A.; Li, L. J. *Adv. Mater.* **2008**, *20*, 2389.

(9) (a) Singh, R.; Premkumar, T.; Shin, J. Y.; Geckeler, K. E. *Chem.—Eur. J.* **2010**, *16*, 1728. (b) Peng, X.; Chen, J.; Misewich, J. A.; Wong, S. S. *Chem. Soc. Rev.* **2009**, *38*, 1076. (c) Georgakilas, V.; Gournis, D.; Tzitzios, V.; Pasquato, L.; Guldi, D. M.; Prato, M. *J. Mater. Chem.* **2007**, *17*, 2679. (d) Wildgoose, G. G.; Banks, C. E.; Compton, R. G. *Small* **2006**, *2*, 182.

(10) Kim, K.; Lee, S. H.; Yi, W.; Kim, J.; Choi, J. W.; Park, Y.; Jin, J. I. *Adv. Mater.* **2003**, *15*, 1618.

(11) Quinn, B. M.; Dekker, C.; Lemay, S. G. *J. Am. Chem. Soc.* **2005**, *127*, 6146.

(12) (a) Moon, S. Y.; Kusunose, T.; Tanaka, S.; Sekino, T. *Carbon* **2009**, *47*, 2924. (b) Xue, B.; Chen, P.; Hong, Q.; Lin, J.; Tan, K. L. *J. Mater. Chem.* **2001**, *11*, 2378.

(13) (a) Ellis, A. V.; Vijayamohanan, K.; Goswami, R.; Chakrapani, N.; Ramanathan, L. S.; Ajayan, P. M.; Ramanath, G. *Nano Lett.* **2003**, *3*, 279. (b) Han, L.; Wu, W.; Kirk, F. L.; Luo, J.; Maye, M. M.; Kariuki, N. N.; Lin, Y.; Wang, C.; Zhong, C. J. *Langmuir* **2004**, *20*, 6019.

(14) (a) Herrero, M. A.; Guerra, J.; Myers, V. S.; Gomez, M. V.; Crooks, R. M.; Prato, M. *ACS Nano* **2010**, *4*, 905. (b) Kim, B.; Sigmund, W. M. *Langmuir* **2004**, *20*, 8239. (c) Wang, Z.; Li, M.; Zhang, Y.; Yuan, J.; Shen, Y.; Niu, L.; Ivaska, A. *Carbon* **2007**, *45*, 2111.

(15) Rance, G. A.; Marsh, D. H.; Bourne, S. J.; Reade, T. J.; Khlobystov, A. N. *ACS Nano* **2010**, *4*, 4920.

(16) Liu, L.; Wang, T.; Li, J.; Guo, Z. X.; Dai, L.; Zhang, D.; Zhu, D. *Chem. Phys. Lett.* **2003**, *367*, 747.

(17) (a) Peng, Z.; Holm, A. H.; Nielsen, L. T.; Pedersen, S. U.; Daasbjerg, K. *Chem. Mater.* **2008**, *20*, 6068. (b) Zanella, R.; Basiuk, E. V.; Santiago, P.; Basiuk, V. A.; Mireles, E.; Puente-Lee, I.; Saniger, J. M. *J. Phys. Chem. B* **2005**, *109*, 16290. (c) Coleman, K. S.; Bailey, S. R.; Fogden, S.; Green, M. L. H. *J. Am. Chem. Soc.* **2003**, *125*, 8722.

(18) Balasubramanian, K.; Burghard, M. *Small* **2005**, *1*, 180.

(19) (a) Chen, J.; Rao, A. M.; Lyuksyutov, S.; Itkis, M. E.; Hamon, M. A.; Hu, H.; Cohn, R. W.; Eklund, P. C.; Colbert, D. T.; Smalley, R. E.; Haddon, R. C. *J. Phys. Chem. B* **2001**, *105*, 2525. (b) Zhang, J.; Zou, H.; Qing, Q.; Yang, Y.; Li, Q.; Liu, Z.; Guo, X.; Du, Z. *J. Phys. Chem. B* **2003**, *107*, 3712. (c) Fasi, A.; Palinko, I.; Seo, J. W.; Konya, Z.; Hernadi, K.; Kiricsi, I. *Chem. Phys. Lett.* **2003**, *372*, 848. (d) Ajayan, M.; Ebbesen, T. W.; Ichihashi, T.; Iijima, S.; Tanigaki, K.; Hiura, H. *Nature* **1993**, *362*, 522. (e) Tsang, S. C.; Harris, P. J. F.; Green, M. L. H. *Nature* **1993**, *362*, 520.

(20) (a) Chen, J.; Hamon, M. A.; Hu, H.; Chen, Y.; Rao, A. M.; Eklund, P. C.; Haddon, R. C. *Science* **1998**, *282*, 95. (b) Chen, Y.; Haddon, R. C.; Fang, S.; Rao, A. M.; Eklund, P. C.; Lee, W. H.; Dickey, E. C.; Grulke, E. A.; Pendergrass, J. C.; Chavan, A.; Haley, B. E.; Smalley, R. E. *J. Mater. Res.* **1998**, *13*, 2423. (c) Holzinger, M.; Vostrowsky, O.; Hirsch, A.; Hennrich, F.; Kappes, M.; Weiss, R.; Jellen, F. *Angew. Chem., Int. Ed.* **2001**, *40*, 4002. (d) Moghaddam, M. J.; Taylor, S.; Gao, M.; Huang, S.; Dai, L.; McCall, M. J. *Nano Lett.* **2004**, *4*, 89. (e) Li, G.; Wang, H.; Zheng, H.; Bai, R. *Langmuir* **2010**, *26*, 7529.

(21) Ismaili, H.; Lee, S.; Workentin, M. S. *Langmuir* **2010**, *26*, 14958.

(22) Brust, M.; Fink, J.; Bethella, D.; Schiffrin, D. J.; Kielyb, C. *J. Chem. Soc., Chem. Commun.* **1995**, 1655.

(23) Manna, A.; Chen, P. L.; Akiyama, H.; Wei, T. X.; Tamada, K.; Knol, W. *Chem. Mater.* **2003**, *15*, 20.

(24) Kotiaho, A.; Lahtinen, R.; Efimov, A.; Metsberg, H. K.; Sariola, E.; Lehtivuori, H.; Tkachenko, N. V.; Lemmetyinen, H. *J. Phys. Chem. C* **2010**, *114*, 162.

(25) Tzitzios, V.; Georgakilas, V.; Oikonomou, E.; Karakassides, M.; Petridis, D. *Carbon* **2006**, *44*, 848.

(26) (a) Behler, K.; Osswald, S.; Ye, H.; Dimovski, S.; Gogosti, Y. *J. Nanopart. Res.* **2006**, *8*, 615. (b) Osswald, S.; Havel, M.; Gogotsi, Y. *J. Raman Spectrosc.* **2007**, *38*, 728.

(27) Felidj, N.; Aubard, J.; Levi, G. *Phys. Rev. B* **2002**, *65*, 0754191.

(28) Wang, T.; Hu, X.; Qu, X.; Dong, S. *J. Phys. Chem. B* **2006**, *110*, 6631.